© 2020 Chinese Physical Society and IOP Publishing Ltd Printed in China and the UK Communications in Theoretical Physics

Commun. Theor. Phys. 72 (2020) 025303 (8pp) https://doi.org/10.1088/1572-9494/ab6906

Nuclear properties of $Z = 114$ isotopes and shell structure of $^{298}114$

Yanzhao Wang (王艳召)[1,2,3,4], Yonghao Gao (高永浩)[1,2], Jianpo Cui (崔建坡)[1,2] and Jianzhong Gu (顾建中)[3]

[1] Department of Mathematics and Physics, Shijiazhuang Tiedao University, Shijiazhuang 050043, China
[2] Institute of Applied Physics, Shijiazhuang Tiedao University, Shijiazhuang 050043, China
[3] China Institute of Atomic Energy, PO Box 275 (10), Beijing 102413, China
[4] Department of Physics, Royal Institute of Technology (KTH), SE-10691 Stockholm, Sweden

E-mail: yanzhaowang09@126.com and jzgu1963@ciae.ac.cn

Received 21 September 2019, revised 7 January 2020
Accepted for publication 8 January 2020
Published 3 February 2020

Abstract

The two-neutron separation energies (S_{2n}) and α-decay energies (Q_α) of the $Z = 114$ isotopes are calculated by the deformed Skyrme–Hartree–Fock–Bogoliubov (SHFB) approach with the SLy5, T22, T32 and T43 interactions. It is found that the tensor force effect on the bulk properties is weak and the shell closure at $N = 184$ is seen evidently with these interactions by analyzing the S_{2n} and Q_α evolutions with neutron number N. Meanwhile, the single-particle energy spectra of $^{298}114$ are studied using the spherical SHFB approach with these interactions to furthermore examine the shell structure of the magic nucleus $^{298}114$. It is shown that the shell structure is almost not changed by the inclusion of the tensor force in the Skyrme interactions. Finally, by examining the energy splitting of the three pairs of pseudospin partners for the protons and neutrons of $^{298}114$, it is concluded that the pseudospin symmetry of the neutron states is preserved better than that of the proton states and not all of the pseudospin symmetries of the proton and neutron states are influenced by the tensor force.

Keywords: superheavy nuclei, Skyrme–Hartree–Fock–Bogoliubov approach, tensor force, two-neutron separation energies, alpha-decay energies, shell structure, pseudospin symmetry

(Some figures may appear in colour only in the online journal)

1. Introduction

Nowadays study on the structure of superheavy nuclei (SHN) has been a hot subject in nuclear physics [1–11]. In recent years, many superheavy elements and isotopes have been synthesized by the cold fusion reactions with Pb or Bi as targets or by the hot fusion reactions with ^{48}Ca as a projectile [1–5]. So far, ^{294}Og (^{294}118) has been the heaviest nuclide, which was produced via the ^{249}Cf+^{48}Ca reaction in Dubana [3–5]. With the progress on the synthesis of SHN, many theoretical methods for the nuclear structure study were developed [12–39]. They can be divided into the following three categories: the Macroscopic–Microscopic (MM) models [12–16], non-relativistic mean field approaches [16–31] and relativistic mean field approaches [30–39]. Since the existence and stability of SHN are closely associated with shell effects, it is very important to search for the magic numbers in the superheavy mass region, which may be the most important issue for the study of SHN. Nevertheless, the magic numbers extracted from different methods are quite different from each other. It is well known that the Skyrme energy density functional theory is an important non-relativistic mean field approach [16, 20–31] and has been used to investigate the bulk properties and shell structure of SHN [16, 24–31]. By the Skyrme–Hartree–Fock (SHF) approach, the predicted magic numbers are ($Z = 114$, $N = 184$), ($Z = 120$, $N = 172$), and ($Z = 126$, $N = 184$) [16, 24, 31]. Besides the magic numbers, many other properties, such as the Q_α values [16, 26, 28], shape coexistence [16, 28–30], and fission barriers [16, 28–30], have been studied by the SHF theory.

In the Skyrme interaction, the tensor force is an essential ingredient. Recent studies indicate that the Skyrme type tensor force plays an important role in exotic nuclear structures [40–62]. In fact, the tensor force was included when the Skyrme interaction was proposed [63]. But it was usually neglected in later calculations because of its complexity. In order to study the tensor force effect on nuclear structure, in the past decades ones have proposed many sets of the Skyrme interactions including the tensor force, such as the SLy5 + T [60] interaction, the T*IJ* family [61, 62]. Some features in single-particle state evolutions and low energy excitations are described well when the tensor force is included [41–52, 56, 58, 59, 61, 62].

In the 1960s, the island of stability of SHN centered near the double-magic $Z = 114$, $N = 184$ nucleus, was predicted by a MM approach [64]. In subsequent studies the nuclear properties of the $Z = 114$ isotopes have been attracting attention from many researchers [3, 4, 16, 24, 25, 27, 33, 65–67]. Several nuclides of the $Z = 114$ isotopes ($^{285-289}114$) have been synthesized through ^{48}Ca-induced reactions and identified by the α-decay chains [4]. Although the nuclear properties of the $Z = 114$ isotopes were discussed by various theoretical models [16, 24, 25, 27, 33], the influence of the tensor force on them was discussed by only a few papers [65–67]. Thus it is interesting to further study the tensor force effect on the nuclear properties of the $Z = 114$ isotopes. This constitutes the first motivation of this article.

In addition, the pseudospin symmetry is an important character for heavy and superheavy systems. In the late 1960s the pseudospin symmetry of the single-particle energies was discovered in heavy nuclei [68, 69]. At that time, it was found that there was a quasi-degeneracy between the single-nucleon doublets with quantum numbers $(n, l, j = l + 1/2)$ and $(n - 1, l + 2, j = l + 3/2)$, where n, l and j are the single nucleon radial, orbital and total angular momentum quantum numbers, respectively. The quasi-degenerate states were relabeled as pseudospin doublets: ($\tilde{n} = n - 1$, $\tilde{l} = l + 1$, $\tilde{j} = l \pm 1/2$). Since the discovery of the pseudospin symmetry, many studies have been done on the subject [70–80]. However, the tensor force was not considered in those studies. Recently, we discussed the tensor force effect on the pseudospin orbital splittings in the Sn isotopes by the Skyrme–Hartree–Fock–Bogoliubov (SHFB) approach with 36 sets of the T*IJ* interactions [81]. Thus, it is important to extend our method to investigate the pseudospin symmetry of the SHN, which might be helpful for deepening our understanding of the SHN structure. This is the second motivation of our article.

Driven by the two above mentioned motivations, firstly we will study the nuclear properties of the $Z = 114$ isotopes, and then discuss the shell structure and pseudospin symmetry by taking $^{298}114$ as an example by employing the SHFB method with the tensor force. This article is organized as follows. In section 2, the theoretical framework is presented. The numerical results and corresponding discussions are given in section 3. In the last section, some conclusions are drawn.

2. Theoretical method

For the nuclear many-body physics, its fundamental task is to understand the nuclear structures and reactions by the many-body calculation starting from the nucleon–nucleon interaction (nuclear force). The modern nuclear force usually refers to the bare nuclear force (for instance, Argonne $v18(95)$ [82] and Reid(93) [83]), the meson exchange potential [84–88] and the potential from low-energy quantum chromodynamics via chiral effective field theory [89, 90]. Nevertheless, the phenomenological nuclear force still plays an important role in the nuclear many-body calculations. The Skyrme force is one kind of phenomenological nuclear forces, by which many properties of stable and unstable nuclei can be described successfully [20–31].

In the framework of the SHFB theory, the total energy E of a nucleus can be modeled by an energy density functional that is the sum of the kinetic, usual Skyrme, pairing, Coulomb and tensor terms

$$\begin{aligned} E &= K + E_{\mathrm{Skyrme}} + E_{\mathrm{Pair}} + E_{\mathrm{Coul}} + E_{\mathrm{Tensor}} \\ &= \int \mathrm{d}^3 r\, [k(\boldsymbol{r}) + \varepsilon_{\mathrm{Skyrme}}(\boldsymbol{r}) + \varepsilon_{\mathrm{Pair}}(\boldsymbol{r}) \\ &\quad + \varepsilon_{\mathrm{Coul}}(\boldsymbol{r}) + \varepsilon_{\mathrm{Tensor}}(\boldsymbol{r})]. \end{aligned} \tag{1}$$

The kinetic, Skyrme, pairing and Coulomb energy densities in equation (1) can be found from [61–63]. Here we only introduce the time even-part of the energy density functional with the inclusion of the tensor force.

The Skyrme type tensor terms are expressed as [61–63]

$$\begin{aligned} v^t(\boldsymbol{r}) = &\frac{1}{2} t_{\mathrm{e}} \{[3(\boldsymbol{\sigma}_1 \cdot \boldsymbol{k}')(\boldsymbol{\sigma}_2 \cdot \boldsymbol{k}') - (\boldsymbol{\sigma}_1 \cdot \boldsymbol{\sigma}_2)\boldsymbol{k}'^2]\delta(\boldsymbol{r}) \\ &+ \delta(\boldsymbol{r})[3(\boldsymbol{\sigma}_1 \cdot \boldsymbol{k})(\boldsymbol{\sigma}_2 \cdot \boldsymbol{k}) - (\boldsymbol{\sigma}_1 \cdot \boldsymbol{\sigma}_2)\boldsymbol{k}^2]\} \\ &+ t_{\mathrm{o}}[3(\boldsymbol{\sigma}_1 \cdot \boldsymbol{k}')\delta(\boldsymbol{r})(\boldsymbol{\sigma}_2 \cdot \boldsymbol{k}) \\ &- (\boldsymbol{\sigma}_1 \cdot \boldsymbol{\sigma}_2)\boldsymbol{k}' \cdot \delta(\boldsymbol{r})\boldsymbol{k}], \end{aligned} \tag{2}$$

where we use the shorthand notation $\boldsymbol{r} = \boldsymbol{r}_1 - \boldsymbol{r}_2$ for the relative position vector between the two particles. The operator for relative momenta $\boldsymbol{k} = (\nabla_1 - \nabla_2)/2\mathrm{i}$ acts on the right and $\boldsymbol{k}' = -(\nabla_1 - \nabla_2)/2\mathrm{i}$ acts on the left. The coupling constants t_{e} and t_{o} are the strengths of the triplet-even and triple-odd tensor interactions, respectively.

For a deformed system, the energy density functional with the tensor force is more complicated than the one for a spherical nucleus. For the ground state of even–even nuclei, the tensor force contribution to the energy density from the time-odd part is zero. Thus, just the time-even tensor term is considered, which can be expressed as [62]

$$\begin{aligned} \varepsilon_{\mathrm{Tensor}}(\boldsymbol{r}) = &C_{\mathrm{t}}^{J0}(J_{\mathrm{t}}^{(0)})^2 \\ &+ C_{\mathrm{t}}^{J1}\boldsymbol{J}_{\mathrm{t}}^2 + C_{\mathrm{t}}^{J2}\textstyle\sum_{\mu,\nu=x}^{z} J_{\mathrm{t},\mu\nu}^{(2)} J_{\mathrm{t},\mu\nu}^{(2)}, \end{aligned} \tag{3}$$

where $J_{\mathrm{t}}^{(0)}$, $\boldsymbol{J}_{\mathrm{t}}$ and $J_{\mathrm{t},\mu\nu}^{(2)}$ represent the pseudoscalar, vector and pseudotensor spin-current tensor densities, respectively. C_{t}^{J0}, C_{t}^{J1} and C_{t}^{J2} are the coupling constants for the three terms (isoscalar $t = 0$, isovector $t = 1$). The tensor terms of the existing Skyrme parameterizations have been adjusted for spherical nuclei, where the time-reversal invariance is kept

Table 1. The SLy5, T22, T32 and T43 parameter sets.

Parameters	SLy5 [91]	T22 [61]	T32 [61]	T43 [61]
t_0 (MeV fm^3)	−2484.88	−2484.40	−2486.16	−2490.28
t_1 (MeV fm^5)	483.13	484.50	489.07	494.61
t_2 (MeV fm^5)	−549.40	−471.45	−438.57	−255.53
t_3 (MeV fm^4)	13 673.00	13 786.97	13 804.97	13 847.12
x_0	0.778	0.730	0.712	0.699
x_1	−0.328	−0.443	−0.499	−0.782
x_2	−1.000	−0.945	−0.912	−0.646
x_3	1.267	1.188	1.160	1.136
W_0 (MeV fm^3)	126.00	123.23	133.59	153.10
σ	1/6	1/6	1/6	1/6
t_e (MeV fm^5)	—	118.69	204.35	196.87
t_o (MeV fm^5)	—	−72.50	−77.18	−49.16

and the second term is the only nonzero term in equation (3). Thus, C_t^{J0} and C_t^{J2} have not been fixed by these fits and one has to make additional choices when studying the deformed system. Reference [62] pointed out that the choices for the values of C_t^{J0} and C_t^{J2} are not unique. Recent work showed that the pseudoscalar and pseudotensor terms are not important for the energy densities [65]. So only the vector part is taken into account in calculations. In the vector part, the coupling constants α and β are used to characterize the interaction strengths of the like-particle $\boldsymbol{J}_t^2$ term and the proton–neutron $\boldsymbol{J}_t^2$ term, respectively [61, 62]

$$\alpha = 2(C_0^{J1} + C_1^{J1}),$$
$$\beta = 2(C_0^{J1} - C_1^{J1}). \quad (4)$$

In equation (4), the coupling constants $\alpha = \alpha_C + \alpha_T$ and $\beta = \beta_C + \beta_T$ can again be separated into the contributions from the central and tensor forces [61–63, 91]

$$\alpha_C = \frac{1}{8}(t_1 - t_2) - \frac{1}{8}(t_1x_1 + t_2x_2),$$
$$\beta_C = -\frac{1}{8}(t_1x_1 + t_2x_2), \quad (5)$$

$$\alpha_T = \frac{5}{4}t_o,$$
$$\beta_T = \frac{5}{8}(t_e + t_o). \quad (6)$$

If the pseudoscalar and pseudotensor contributions are neglected, the spin–orbit potential can be written as

$$W_{q,\mu\nu}(\boldsymbol{r}) = -b_9\sum_{k=x}^{z} \epsilon_{k\mu\nu}(\nabla_k\rho + \nabla_k\rho_q) + 2b_{14}J_{\mu\nu} + 2b_{15}J_{q,\mu\nu}, \quad (7)$$

where the constant $b_9 = -\frac{W_0}{2}$. The coupling constants b_{14} and b_{15} can be obtained by the equations (12), (17) of [62] combining the appendix A of [61]. In the expression q stands for protons and neutrons $q = p, n$.

Besides the mean-field, the pairing correlation plays a significant role in the SHN structure. In the pairing channel, a widely used density-dependent δ interaction is employed, which is expressed as

$$V_{\text{pair}}(\boldsymbol{r} - \boldsymbol{r}') = V_0\left(1 - \frac{1}{2}\frac{\rho(\boldsymbol{r})}{\rho_0}\right)\delta(\boldsymbol{r} - \boldsymbol{r}'), \quad (8)$$

where V_0 is the pairing strength parameter, which is fitted to the mean neutron gap (1.31 MeV) of ^{120}Sn. $\rho(\boldsymbol{r})$ is the isoscalar local density, and ρ_0 is the nuclear matter saturation density fixed at 0.16 fm^{-3}.

3. Results and discussions

In this work, the calculations on the bulk properties are performed firstly by the HTBTHO code [22] with the SLy5 [91], T22, T32 and T43 forces [61] and zero-range paring interaction. Note that the T22, T32 and T43 forces include the tensor component and the SLy5 interaction does not. The four sets of parameterizations are listed in table 1. The work of Bai *et al* suggested that the T22, T32 and T43 interactions can reproduce the experimental data of the charge exchange spin dipole excitation of ^{208}Pb by a self-consistent SHF based random phase approximation [56]. Therefore, in this article, the T22, T32 and T43 interactions are used. Some studies showed the collapse of pairing at large shell gaps in spherical SHN in the self-consistent calculations performed either in an approximate Hartree–Fock+BCS or a full Hartree–Fock–Bogoliubov framework [92, 93]. The principal shortcoming of these calculations is the fact that neither the BCS nor the HFB wave functions are the eigenstates of the particle number operator [94]. The best way to deal with this problem would be to perform an exact particle number projection (PNP) before the variation [94], but this is very time-consuming for realistic interactions. A relevant study indicates that an approximate PNP by means of the Lipkin–Nogami (LN) method removes the pairing collapse seen at large shell gaps in spherical SHN in the calculations without PNP [95]. Thus, in the calculations of this work, the LN correction is considered. Besides the LN correction, in calculations we employ the harmonic oscillator (HO) basis. For the HO basis

Table 2. The S_{2n} values of the $Z = 114$ isotopes with the SLy5, T22, T32 and T43 interactions and the WS4 mass table. The S_{2n} values are measured in MeV.

Nuclei	S_{2n} (SLy5)	S_{2n} (T22)	S_{2n} (T32)	S_{2n} (T43)	S_{2n} (WS4)
$^{274}114$	16.27	16.38	16.30	16.34	17.03
$^{276}114$	15.80	15.92	15.84	15.79	16.67
$^{278}114$	15.04	15.16	15.11	15.03	15.67
$^{280}114$	14.32	14.43	14.40	14.29	15.10
$^{282}114$	13.69	13.77	13.78	13.66	14.81
$^{284}114$	13.60	13.60	13.69	13.65	14.52
$^{286}114$	13.09	13.19	13.19	13.07	13.86
$^{288}114$	12.43	12.69	12.67	12.84	13.40
$^{290}114$	12.68	12.87	12.79	12.74	12.79
$^{292}114$	12.07	12.19	12.19	12.07	12.47
$^{294}114$	11.60	11.90	11.77	11.78	11.71
$^{296}114$	11.34	11.45	11.59	11.34	11.25
$^{298}114$	10.91	11.18	11.24	11.26	10.64
$^{300}114$	7.45	7.54	7.68	7.68	8.53
$^{302}114$	7.28	7.34	7.48	7.48	8.25
$^{304}114$	8.46	8.35	8.47	8.36	8.72
$^{306}114$	9.06	8.98	8.81	8.58	8.88
$^{308}114$	8.64	8.78	8.80	8.74	8.88
$^{310}114$	8.32	8.40	8.43	8.35	9.01
$^{312}114$	7.90	8.04	8.07	7.95	8.50
$^{314}114$	7.57	7.66	7.69	7.61	8.21
$^{316}114$	7.25	7.36	7.40	7.27	7.58
$^{318}114$	6.92	7.04	7.08	7.00	7.06
$^{320}114$	6.61	6.74	6.76	6.67	6.98
$^{322}114$	6.37	6.49	6.51	6.47	6.89
$^{324}114$	6.06	6.55	6.53	6.51	6.78
$^{326}114$	5.97	6.23	6.25	6.16	6.38
$^{328}114$	5.77	5.95	5.95	5.87	6.05
$^{330}114$	5.44	5.57	5.61	5.53	5.84
$^{332}114$	5.21	5.30	5.35	5.30	5.35
$^{334}114$	4.91	5.07	5.07	4.99	5.13

parameter b_0 ($b_0 < 0$), the code uses the default value of $b_0 = \sqrt{2(\hbar^2/2m)/(41fA^{-1/3})}$ for $f = 1.2$. The number of oscillator shells is taken to be $N_{\max} = 20$. In the pairing channel, the fitted V_0 values are -344.82, -342.81, -342.61 and -339.48 MeV fm^3 for the SLy5, T22, T32 and T43 interactions, respectively. The quasi-particle cut-off energy is 60 MeV. All calculations of this article are converged with the above conditions.

Firstly, the S_{2n} values of the $Z = 114$ isotopes have been calculated with the four sets of parameterizations, which are shown in table 2. From table 2, it is seen that the S_{2n} values with the SLy5 interaction are close to those with the T22, T32 and T43 interactions, which indicates that the tensor terms in the T22, T32 and T43 interactions have a little influence on the bulk properties of SHN. To test the calculated accuracies for these interactions, the S_{2n} values extracted from the WS4 mass model are also given in table 2 considering the rms deviation with respect to the 2353 known masses given by the WS4 model falls within 298 keV [13, 14]. As to the S_{2n} values, the extracted rms deviations between those given by the SHFB approach with the four interactions and by the WS4 model are 0.60, 0.52, 0.50 and 0.54, respectively. This suggests that the accuracy of S_{2n} values is improved slightly by including the tensor force. To reveal the nuclear structure information clearly, the S_{2n} values as functions of N are plotted in figure 1, in which a pronounced kink appears at $N = 184$ with these interactions and the WS4 model, indicating that 184 is a neutron magic number.

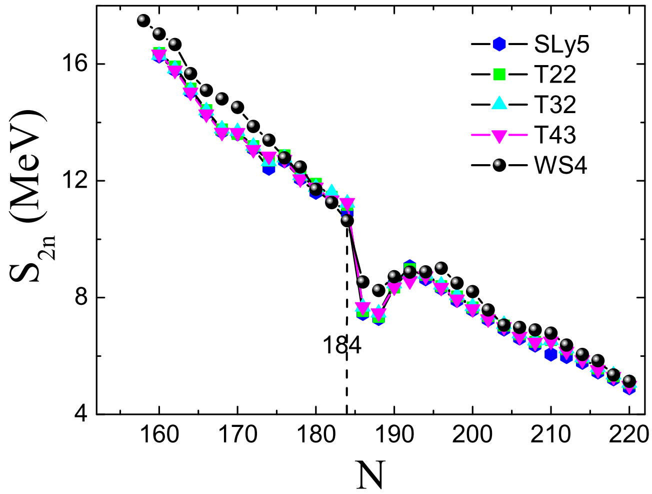

Figure 1. The S_{2n} values of the $Z = 114$ isotopes versus neutron number N by the SLy5, T22, T32 and T43 interactions. The filled circles represent the S_{2n} values extracted from the WS4 mass model [13, 14].

For SHN, α-decay is one of the important decay modes [1–11]. In recent years, many SHN have been produced by hot and cold fusion reactions and their Q_α values have been measured [3–5]. In fact, these experimental Q_α values are significant for testing various nuclear mass models. Relevant studies indicate that the predicted ability of MM approach is the most powerful in the description of nuclear masses [96, 97]. Furthermore, our recent work suggests that one kind of MM models, the WS4 model, is the most accurate one to reproduce the experimental Q_α values [9]. In table 3, the Q_α values of the $Z = 114$ isotopes by the deformed SHFB method and WS4 model are therefore listed. For the even–even nuclei of the $Z = 114$ isotopes, only $^{286}114$ and $^{288}114$ were identified by α-particle emissions [3, 4]. So, in table 3 their experimental Q_α values are given. As can be seen from table 3, the deviation between the experimental Q_α values and those from the WS4 model is just about 0.25, which is smaller than the deviation between the experimental data and SHFB calculations. Thus, the accuracy by the WS4 mass model is higher than that by the SHFB approach. This conclusion is consistent with that of our recent work [9]. In addition, the theoretical and experimental Q_α values are plotted in figure 2 where one can see that the evident shell closure effect is at $N = 184$ for all the models. The submagic shell at $N = 162$ is seen only for the WS4 model.

Since the neutron magic nucleus has a spherical shape, we will discuss the tensor force effect on the single-particle energy spectra of $^{298}114$ by the spherical HFBRAD code [23]. In the calculations the spherical box and mesh sizes are selected as 30 fm and 0.1 fm, respectively. The quasi-particle

Table 3. Same as table 1, but for the Q_α values. The Q_α values are measured in MeV.

Nuclei	Q_α (SLy5)	Q_α (T22)	Q_α (T32)	Q_α (T43)	Q_α (WS4)	Q_α (Expt.)
$^{272}114$	13.28	13.32	13.31	13.22	13.16	
$^{274}114$	13.03	13.04	13.08	12.90	12.78	
$^{276}114$	12.66	12.66	12.71	12.54	12.32	
$^{278}114$	12.33	12.31	12.36	12.26	12.52	
$^{280}114$	12.24	12.23	12.28	12.21	12.23	
$^{282}114$	12.10	12.15	12.15	12.10	11.38	
$^{284}114$	11.44	11.54	11.48	11.34	10.57	
$^{286}114$	10.79	10.81	10.83	10.74	9.97	10.21 ±0.04 [4]
$^{288}114$	10.73	10.58	10.63	10.26	9.65	9.93 ±0.03 [4]
$^{290}114$	9.78	9.63	9.75	9.55	9.52	
$^{292}114$	9.51	9.54	9.58	9.49	8.95	
$^{294}114$	9.31	9.17	9.34	9.12	8.71	
$^{296}114$	8.98	8.86	8.88	8.84	8.56	
$^{298}114$	7.99	7.89	8.11	8.18	8.27	
$^{300}114$	10.96	11.06	11.19	11.26	9.56	
$^{302}114$	10.46	10.58	10.71	10.76	9.29	
$^{304}114$	9.08	9.54	9.47	9.17	8.43	
$^{306}114$	7.69	8.27	8.49	8.28	8.26	
$^{308}114$	7.47	7.61	7.61	7.46	7.77	
$^{310}114$	7.23	7.42	7.39	7.24	7.47	
$^{312}114$	7.09	7.19	7.17	7.03	7.39	
$^{314}114$	6.85	6.95	6.94	6.83	7.14	
$^{316}114$	6.58	6.76	6.72	6.58	7.28	
$^{318}114$	6.33	6.50	6.47	6.30	7.32	
$^{320}114$	6.11	6.29	6.25	6.15	6.80	
$^{322}114$	5.79	6.30	6.30	6.20	6.10	
$^{324}114$	5.91	6.06	6.10	5.94	5.47	
$^{326}114$	5.80	5.86	5.87	5.73	5.38	
$^{328}114$	5.55	5.61	5.63	5.51	5.22	
$^{330}114$	5.34	5.40	5.40	5.29	4.89	
$^{332}114$	5.02	5.14	5.12	4.98	4.90	
$^{334}114$	4.67	4.81	4.80	4.64	4.54	

energies are cut off at 60 MeV. The maximum angular momentum of the quasiparticles $j_{\max}$ is set to be $\frac{39}{2}\hbar$. Because the nuclear properties are mainly determined by the single-particle orbitals near the Fermi levels, the proton and neutron single-particle energy spectra of $^{298}114$ near the Fermi levels by the SLy5, T22, T32 and T43 interactions are showed in figures 3 and 4. From the single-proton energy spectrum by the SLy5 interaction in figure 3, some proton energy gaps can be seen evidently at $Z = 82$, 92, 114, 126, 138 and 164. Furthermore, the energy gap at $Z = 114$ is much smaller than those at $Z = 82$, 92, 126, 138 and 164. Therefore, $Z = 114$ could be seen as a submagic number. As to the cases of the T22, T32 and T43 interactions, some orbitals are pulled up or pushed down slightly. The mechanism for the orbital shift can be found in [44, 45]. In addition, the predicted level orderings by the three TIJ interactions remain unchanged and the predicted energies and gaps are not changed significantly by comparing to those by the SLy5 interaction, which suggests

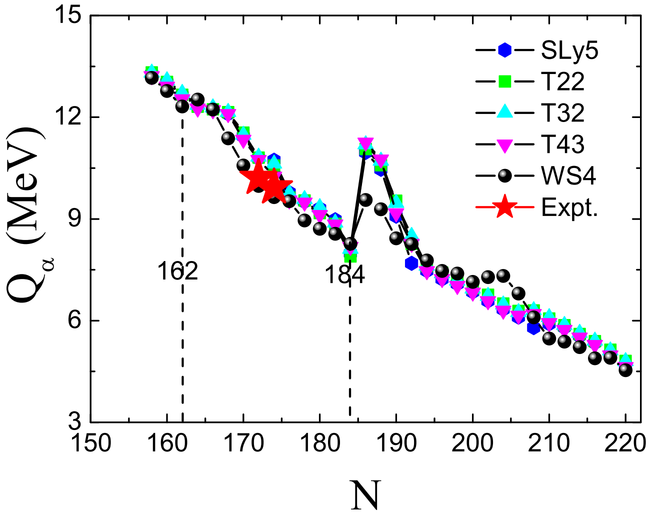

Figure 2. The Q_α values of the $Z = 114$ isotopes versus N by the SLy5, T22, T32 and T43 interactions. The filled circles represent the Q_α values extracted from the WS4 mass model [13, 14]. The experimental Q_α values of $^{286,288}114$ are taken from [3, 4] and marked with the red stars.

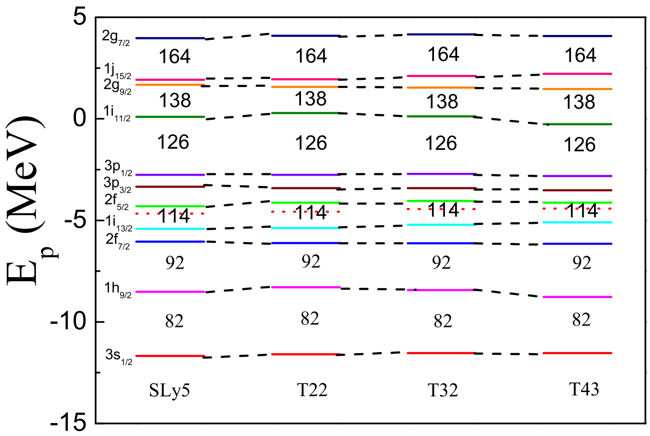

Figure 3. The single-proton energy spectra of $^{298}114$ near the Fermi levels by the SLy5, T22, T32 and T43 interactions. The red dot lines denote the Fermi levels. The same orbitals are linked with the black dashed lines.

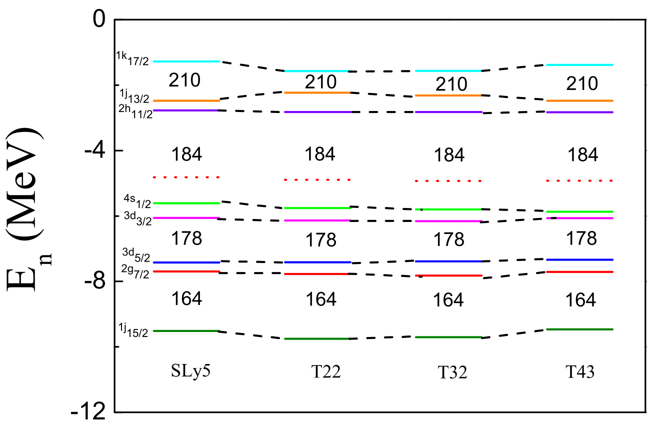

Figure 4. Same as figure 3, but for the single-neutron energy spectra.

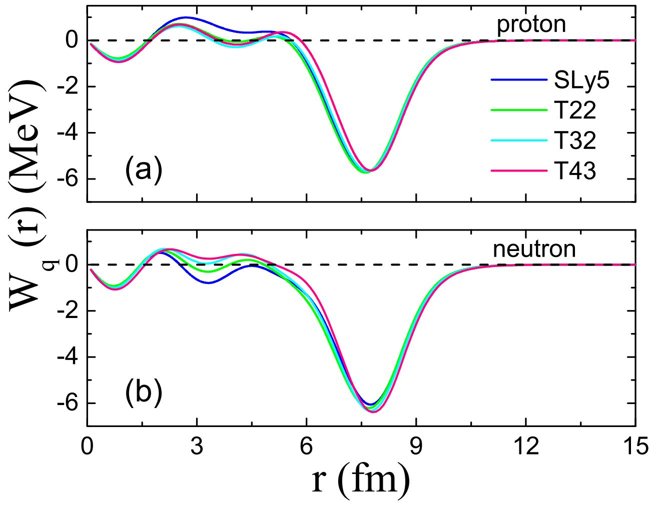

Figure 5. The proton and neutron spin–orbit potentials of ^{298}114 by the SLy5, T22, T32 and T43 interactions.

that the energy spectra of ^{298}114 are almost not influenced by the tensor force. The reason may be due to the spin–orbit potential, hence the proton spin–orbit potentials with the SLy5, T22, T32 and T43 interactions are shown in figure 5(a). From figure 5(a), it is observed that the spin–orbit potential profile with the SLy5 interaction is nearly identical to the ones with the three T*IJ* interactions. Thus, the tensor force contribution to the spin–orbit potential is small. As a result, the single-proton energy spectra are not modified largely by the tensor force.

For the neutron energy spectra, a similar conclusion can be obtained from figure 4. But the shell structure at neutron magic numbers $N = 164$, 178 and 184 can be seen clearly for the four interactions. For the energy gap at $N = 210$, the results by the SLy5 and T43 interactions are a little more noticeable than those by the T22 and T32 interactions. The reason can also be explained by the neutron spin–orbit potential shown in figure 5(b). Combining figure 5 of this article and the conclusions drawn in our work about the tensor force effect on the light nuclei [44, 45], one can understand qualitatively the tensor force contribution to the nuclear structure as follows: the mean-field of a nucleus with $Z = 114$ is much more well-behaved than that of a light nucleus being much more nucleons in it. In a nucleus with $Z = 114$, the contribution by the tensor force to the spin–orbit potential is much smaller compared with the contribution by the whole mean-field. As a result, the tensor effect on the single-particle energy spectra is slight. Furthermore, the bulk properties of the $Z = 114$ isotopes are almost not changed by the tensor force. Thus, the tensor force effect can be observed more easily in light nuclei. Searching for the tensor force effect of light nuclei was carried out by some experimental researchers [98].

From the pseudospin symmetry perspective, it is difficult to judge whether the pseudospin symmetry is kept or not because the single-particle energies are not well-distributed. For single nucleon energy spectra, the energy level density increases with energy rapidly. In our recent work, a criterion judging the pseudospin symmetry breaking was proposed [81]. To describe conveniently, it can be written as

$$c = \frac{\Delta\varepsilon}{\bar{s}}, \tag{9}$$

where $\Delta\varepsilon$ is the energy difference between a pair of pseudospin partners, and $\bar{s}$ is the mean energy level spacing around the pair of pseudospin partners. Note that the energy gaps at the magic and submagic numbers are not taken into account in the $\bar{s}$ calculation. We define that if $c>1$, the symmetry is kept. Otherwise, the symmetry is broken.

Table 4. The proton pseudospin orbital splittings and pseudospin doublets of the $1\tilde{g}$ ($2f_{7/2}$-$1h_{9/2}$), $2\tilde{d}$ ($3p_{3/2}$-$2f_{5/2}$), and $1\tilde{h}$ ($2g_{9/2}$-$1i_{11/2}$) of ^{298}114 by the SLy5, T22, T32 and T43 interactions.

Skyrme interactions	$\Delta\varepsilon$(MeV)	$\bar{s}$(MeV)	c	Symmetry
		$1\tilde{g}$ ($2f_{7/2}-1h_{9/2}$)		
SLy5	2.462	1.549	1.589	N
T22	2.174	1.459	1.490	N
T32	2.303	1.610	1.430	N
T43	2.623	1.839	1.426	N
		$2\tilde{d}$ ($3p_{3/2}-2f_{5/2}$)		
SLy5	0.961	0.776	1.238	N
T22	0.716	0.685	1.045	N
T32	0.635	0.668	0.951	Y
T43	0.604	0.654	0.924	Y
		$1\tilde{h}$ ($2g_{9/2}-1i_{11/2}$)		
SLy5	1.587	0.912	1.740	N
T22	1.286	0.828	1.553	N
T32	1.424	0.997	1.428	N
T43	1.726	1.238	1.394	N

In table 4 we list the proton pseudospin orbital splittings and pseudospin doublets of $1\tilde{g}$ ($2f_{7/2}$-$1h_{9/2}$), $2\tilde{d}$ ($3p_{3/2}-2f_{5/2}$), and $1\tilde{h}$ ($2g_{9/2}-1i_{11/2}$) of ^{298}114 by the SLy5, T22, T32 and T43 interactions. In the last column of table 4, 'Y' represents the pseudospin symmetry is preserved. On the contrary, 'N' means the symmetry is broken. As can be seen from table 4, the symmetries of $1\tilde{g}$ and $1\tilde{h}$ doublets are not kept for the SLy5 interaction. And the symmetry breaking of the two doublets can not be recovered by the T22, T32 and T43 interactions. For the case of the $2\tilde{d}$ doublet, its symmetry is broken by the SLy5 interaction. However, the T32 and T43 interactions restore its symmetry but the T22 interaction does not. According to the above discussion, it is not difficult to see that not all of the pseudospin symmetries are influenced by the tensor force. In other words, the pseudospin symmetry is dependent on the type of the Skyrme interactions used even though the tensor force is taken into account.

For the case of the neutron pseudospin orbital splittings, the pseudospin doublets $2\tilde{f}$ ($2g_{7/2}$-$3d_{5/2}$), $3\tilde{p}$ ($3d_{3/2}$-$4s_{1/2}$), and $1\tilde{i}$ ($2h_{11/2}$-$1j_{13/2}$) are listed in table 5. By analyzing the results of table 5, it is seen that the symmetries of the pseudospin neutron states are not broken by the tensor force.

Table 5. Same as table 3, but for the pseudospin neutron doublets $2\tilde{f}$ $(2g_{7/2}-3d_{5/2})$, $3\tilde{p}$ $(3d_{3/2}-4s_{1/2})$, and $1\tilde{i}$ $(2h_{11/2}-1j_{13/2})$.

Skyrme interactions	$\Delta\varepsilon$ (MeV)	$\bar{s}$(MeV)	c	Symmetry
		$2\ \tilde{f}\ (2g_{7/2}\text{-}3d_{5/2})$		
SLy5	0.271	0.695	0.390	Y
T22	0.360	0.673	0.545	Y
T32	0.433	0.673	0.643	Y
T43	0.374	0.614	0.609	Y
		$3\ \tilde{p}\ (3d_{3/2}\text{-}4s_{1/2})$		
SLy5	0.451	0.695	0.649	Y
T22	0.383	0.673	0.569	Y
T32	0.360	0.673	0.535	Y
T43	0.198	0.614	0.322	Y
		$1\ \tilde{i}\ (2h_{11/2}\text{-}1j_{13/2})$		
SLy5	0.289	0.746	0.387	Y
T22	0.593	0.627	0.946	Y
T32	0.507	0.627	0.809	Y
T43	0.351	0.724	0.485	Y

Furthermore, the symmetries of the pseudospin neutron states are kept better than those of the pseudospin proton states.

4. Conclusions

In this article the S_{2n} and Q_α values of the $Z = 114$ isotopes have been extracted firstly by the deformed SHFB approach with the SLy5, T22, T32 and T43 interactions. Then, the calculated S_{2n} and Q_α values have been compared with the results by the WS4 model and the extant experimental Q_α values. At last, the shell structure and pseudospin splitting of $^{298}114$ have been studied by the spherical SHFB approach. The calculated results allow us to draw the following conclusions:

(i) The predicted accuracy is improved slightly by the tensor force although the tensor force contribution to the S_{2n} values is small.
(ii) The experimental Q_α values are reproduced better with the WS4 model by comparing with the results with the SHFB approach.
(iii) For each interaction, the shell closure at $N = 184$ can be seen evidently by analyzing the S_{2n} and Q_α evolutions with N and the single-neutron energy spectra.
(iv) The single-nucleon energy spectra are almost not influenced by the tensor force and it is not easy to observe the tensor force effect in the nuclear ground state of $Z = 114$ isotopes.
(v) The pseudospin symmetry is dependent on the type of the Skyrme interactions with the tensor force. Moreover, the neutron pseudospin symmetries are preserved better than the proton ones.

However, it is necessary to point out that only the three sets of Skyrme interactions including the tensor force are used in this article. In fact, there exist 40 more sets of the Skyrme parameterizations with the tensor force [60–62, 42, 53–55]. Our previous studies suggested that the tensor force contribution to the nuclear structure is dependent on the magnitudes of the tensor force [44–52]. Therefore, it is interesting to further study the the nuclear properties of the $Z = 114$ isotopes by more sets of Skyrme interactions with the tensor components, which is a work in progress.

Acknowledgments

We thank professor Shangui Zhou, professor Fengshou Zhang and Dr Xiaobao Wang for helpful discussions and the anonymous referee for thoughtful suggestions. This work was supported by the National Natural Science Foundation of China (Grants No. U1832120 and No. 11675265), the Natural Science Foundation for Outstanding Young Scholars of Hebei Province of China (Grant No. A2018210146) and the Continuous Basic Scientific Research Project (Grant No. WDJC-2019-13).

References

[1] Hofmann S and Münzenberg G 2000 *Rev. Mod. Phys.* **72** 733
[2] Hofmann S 2009 *Prog. Part. Nucl. Phys.* **62** 337
[3] Oganessian Y T and Utyonkov V K 2015 *Nucl. Phys.* A **944** 62
[4] Oganessian Y T, Sobiczewski A and Ter-Akopian G M 2017 *Phys. Scr.* **92** 023003
[5] Oganessian Y T *et al* 2006 *Phys. Rev.* C **74** 044602
[6] Morita K 2009 *Prog. Part. Nucl. Phys.* **62** 325
[7] Sobiczewski A and Pomorski K 2007 *Prog. Part. Nucl. Phys.* **58** 292
[8] Deng J G, Cheng J H, Zheng B and Li X H 2017 *Chin. Phys.* C **41** 124109
[9] Wang Y Z, Wang S J, Hou Z Y and Gu J Z 2015 *Phys. Rev.* C **92** 064301
[10] Zhang S, Zhang Y L, Cui J P *et al* 2017 *Phys. Rev.* C **95** 014311
[11] Cui J P, Zhang Y L, Zhang S *et al* 2018 *Phys. Rev.* C **97** 014316
[12] Royer G and Rousseau R 2009 *Eur. Phys. J.* A **42** 541
[13] Wang N, Liu M, Wu X Z and Meng J 2014 *Phys. Lett.* B **734** 215
[14] Weizsäcker-Skyrme Nuclear Mass Tables http://imqmd.com/mass/.
[15] Möller P, Sierk A J, Ichikawa T and Sagawa H 2016 *At. Nucl. Data Tables* **109-110** 1
[16] Ćwiok S, Dobaczewski J, Heenen P-H, Magierski P and Nazarewicz W 1996 *Nucl. Phys.* A **611** 211
[17] Chen Y S, Sun Y and Gao Z C 2008 *Phys. Rev.* C **77** 061305
[18] http://phynu.cea.fr/science_en_ligne/carte_potent-iels_microscopiques/carte_potentiel_nucleaire.htm
[19] Koura H and Chiba S 2013 *J. Phys. Soc. Japan* **82** 014201
[20] Bonche P, Flocard H and Heenen P-H 2005 *Comput. Phys. Commun.* **171** 49
[21] Dobaczewski J, Satula W, Carlsson B G *et al* 2009 *Comput. Phys. Commun.* **180** 2361

[22] Stoitsov M V, Dobaczewski J, Nazarewicz W and Ring P 2005 *Comput. Phys. Commun.* **167** 43
[23] Bennaceur K and Dobaczewski J 2005 *Comput. Phys. Commun.* **168** 96
[24] Rutz K *et al* 1997 *Phys. Rev.* C **56** 238
[25] Ismail M, Ellithi A Y, Botros M M and Adel A 2010 *Phys. At. Nucl.* **73** 1660
[26] Typel S and Brown B A 2003 *Phys. Rev.* C **67** 034313
[27] Vautherin D and Brink D M 1972 *Phys. Rev.* C **5** 626
[28] Bender M, Heenen P-H and Reinhard P-G 2003 *Rev. Mod. Phys.* **75** 121
[29] Bender M, Rutz K, Reinhard P-G, Maruhn J A and Greiner W 1998 *Phys. Rev.* C **58** 2126
[30] Bürvenich T, Bender M, Maruhn J A and Reinhard P-G 2004 *Phys. Rev.* C **69** 014307
[31] Bender M, Rutz K, Reinhard P-G, Maruhn J A and Greiner W 1999 *Phys. Rev.* C **60** 034304
[32] Meng J, Toki H, Zhou S G, Zhang S Q, Long W H and Geng L S 2006 *Prog. Part. Nucl. Phys.* **57** 470
[33] Boersma H F 1993 *Phys. Rev.* C **48** 472
[34] Zhang W, Meng J, Zhang S Q, Geng L S and Toki H 2005 *Nucl. Phys.* A **753** 106
[35] Afanasjev A V and Frauendorf S 2005 *Phys. Rev.* C **71** 024308
[36] Agbemava S E, Afanasjev A V, Nakatsukasa T and Ring P 2015 *Phys. Rev.* C **92** 054310
[37] Agbemava S E and Afanasjev A V 2017 *Phys. Rev.* C **96** 024301
[38] Li J J, Long W H, Margueron J and Giai N Van 2014 *Phys. Lett.* B **732** 169
[39] Li J J, Long W H, Margueron J and Van Giai N 2015 *J. Phys.: Conf. Ser.* **580** 012006
[40] Nakada H, Sugiura K and Margueron J 2013 *Phys. Rev.* C **87** 067305
[41] Grasso M, Ma Z Y, Khan E, Margueron J and Giai N Van 2007 *Phys. Rev.* C **76** 044319
[42] Grasso M and Anguiano M 2013 *Phys. Rev.* C **88** 054328
[43] Grasso M 2014 *Phys. Rev.* C **89** 034316
[44] Wang Y Z, Gu J Z, Dong J M and Zhang X Z 2011 *Phys. Rev.* C **83** 054305
[45] Wang Y Z, Gu J Z, Zhang X Z and Dong J M 2011 *Phys. Rev.* C **84** 044333
[46] Wang Y Z, Gu J Z, Li Z Y, Yu G L and Hou Z Y 2013 *Eur. Phys. J.* A **49** 15
[47] Wang Y Z, Gu J Z, Yu G L and Hou Z Y 2014 *Chin. Phys. Lett.* **31** 102102
[48] Wang Y Z, Cao L G, Gu J Z and Hou Z Y 2014 *Int. J. Mod. Phys.* E **23** 1450082
[49] Wang Y Z, Hou Z Y, Q L Zhang, Tian R L and Gu J Z 2015 *Phys. Rev.* C **91** 017302
[50] Wang Y Z, Su X D, Qi C and Gu J Z 2019 *Chin. Phys.* C **43** 114101
[51] Li Z Y, Wang Y Z, Yu G L and Gu J Z 2013 *Sci. Chin: Phys. Mech. Astron.* **56** 1719
[52] Yu G L, Gu J Z, Wang Y Z, Li Z Y and Meng G Q 2014 *Sci. Chin: Phys. Mech. Astron.* **57** 1662
[53] Brown B A, Duguet T, Otsuka T, Abe D and Suzuki T 2006 *Phys. Rev.* C **74** 061303
[54] Brink D M and Stancu F 2007 *Phys. Rev.* C **75** 064311
[55] Zalewski M, Dobaczewski J, Satula W and Werner T R 2008 *Phys. Rev.* C **77** 024316
[56] Bai C L, Zhang H Q, Sagawa H, Zhang X Z, Coló G and Xu F R 2010 *Phys. Rev. Lett.* **105** 072501
[57] Smirnova N A *et al* 2010 *Phys. Lett.* B **686** 109
[58] Cao L G, Coló G, Sagawa H, Bortignon P F and Sciacchitano L 2009 *Phys. Rev.* C **80** 064304
[59] Cao L G, Coló G and Sagawa H 2010 *Phys. Rev.* C **81** 044302
[60] Coló G, Sagawa H, Fracasso S and Bortignon P F 2007 *Phys. Lett.* B **646** 227
Coló G, Sagawa H, Fracasso S and Bortignon P F 2008 *Phys. Lett.* B **668** 457
[61] Lesinski T, Bender M, Bennaceur K, Duguet T and Meyer J 2007 *Phys. Rev.* C **76** 014312
[62] Bender M, Bennaceur K, Duguet T, Heenen P-H, Lesinski T and Meyer J 2009 *Phys. Rev.* C **80** 064302
[63] Skyrme T H R 1959 *Nucl. Phys.* **9** 615
Skyrme T H R 1959 *Nucl. Phys.* **9** 635
[64] Nilsson S G *et al* 1969 *Nucl. Phys.* A **131** 1
[65] Zhou X R and Sagawa H 2012 *J. Phys. G: Nucl. Part. Phys.* **39** 085104
[66] Suckling E B and Stevenson P D 2010 *Europhys. Lett.* **90** 12001
[67] Dong J M, Zuo W, Gu J Z, Wang Y Z, Cao L G and Zhang X Z 2011 *Phys. Rev.* C **84** 014303
[68] Hecht K T and Adler A 1969 *Nucl. Phys.* A **137** 129
[69] Arima A, Harvey M and Shimizu K 1969 *Phys. Lett.* B **30** 517
[70] Bohr A, Hamamoto I and Mottelson B R 1982 *Phys. Scr.* **26** 267
[71] Dudek J, Nazarewicz W, Szymanski Z and Leander G A 1987 *Phys. Rev. Lett.* **59** 1405
[72] Troltenier D, Nazarewicz W, Szymański Z and Draayer J P 1994 *Nucl. Phys.* A **567** 591
[73] Nazarewicz W, Twin P J, Fallon P and Garrett J D 1990 *Phys. Rev. Lett.* **64** 1654
[74] Stephens F S *et al* 1998 *Phys. Rev.* C **57** R1565
[75] Bahri C, Draayer J P and Moszkowski S A 1992 *Phys. Rev. Lett.* **68** 2133
[76] Ginocchio J N 1997 *Phys. Rev. Lett.* **78** 436
Ginocchio J N 1999 *Phys. Rep.* **315** 231
Ginocchio J N 2005 *Phys. Rep.* **414** 165
[77] Meng J, Sugawara-Tanabe K, Yamaji S and Arima A 1999 *Phys. Rev.* C **59** 154
[78] Guo J Y and Fang X Z 2006 *Phys. Rev.* C **74** 024320
[79] Lv B N, Zhao E G and Zhou S G 2012 *Phys. Rev. Lett.* **109** 072501
[80] Liang H Z, Meng J and Zhou S G 2015 *Phys. Rep* **570** 1
[81] Wang Y Z, Yu G L, Li Z Y and Gu J Z 2013 *J. Phys. G: Nucl. Part. Phys.* **40** 045105
[82] Wiringa R B, Stoks V G J and Schiavilla R 1995 *Phys. Rev.* C **51** 38
[83] Stoks V G J, Klomp R A M, Treheggen C P F *et al* 1994 *Phys. Rev.* C **49** 2950
[84] Machleidt R, Sammarruca F and Song Y 1996 *Phys. Rev.* C **53** 1483
[85] Vretenar D, Afanasjev A V, Lalazissis G A and Ring P 2005 *Phys. Rep.* **409** 101
[86] Long W, Meng J, Van Giai N and Zhou S-G 2004 *Phys. Rev.* C **69** 034319
[87] Long W H, Van Giai N and Meng J 2006 *Phys. Lett.* B **640** 150
[88] Long W, Sagawa H, Meng J and Van Giai N 2008 *Europhys. Lett.* **82** 12001
[89] Epelbaum E, Hammer H-W and Meißner U-G 2009 *Rev. Mod. Phys.* **81** 1773
[90] Machleidt R and Entem D R 2011 *Phys. Rep.* **503** 1
[91] Chabanat E, Bonche P, Haensel P, Meyer J and Schaeffer R 1998 *Nucl. Phys.* A **635** 231
[92] Lalazissis G A, Sharma M M, Ring P and Gambhir Y K 1996 *Nucl. Phys.* A **608** 202
[93] Sil T, Patra S K, Sharma B K, Centelles M and Vinas X 2004 *Phys. Rev. C* **69** 044315
[94] Afanasjev A V, Khoo T L, Frauendorf S, Lalazissis G A and Ahmad I *Phys. Rev.* C **67** 024309
[95] Afanasjev A V 2006 *Phys. Scr.* **T125** 62
[96] Sobiczewski A and Litvinov Yu A 2014 *Phys. Rev.* C **89** 024311
Sobiczewski A and Litvinov Yu A 2014 *Phys. Rev.* C **90** 017302
[97] Cui J P, Gao Y H, Wang Y Z and Gu J Z 2020 *Phys. Rev.* C **101** 014301
[98] Tanihata I 2010 *Mod. Phys. Lett.* A **25** 1886
Ong H J *et al* 2013 *Phys. Lett.* B **725** 277